

Selective Catalytic Isomerization of β -Pinene Oxide to Perillyl Alcohol Enhanced by Protic Tetraimidazolium Nitrate

Hui Li, Jian Liu, Juan Zhao, Huiting He, Dabo Jiang, Steven Robert Kirk, Qiong Xu, Xianxiang Liu, and Dulin Yin^{*[a]}

A series of tetraimidazolium salts with different anions was prepared and applied in the isomerization of β -pinene oxide. After examining the activity of different catalysts, a remarkable enhancement of the selectivity of perillyl alcohol (47%) was obtained over [PEimi][HNO₃]₄ under mild reaction conditions

and using DMSO as the solvent. Furthermore, noncovalent interactions between solvent molecules and the catalyst were found by FT-IR spectroscopy and confirmed by computational chemistry. The homogeneous catalyst showed excellent stability and was reused up to six times without significant loss.

1. Introduction

Conversion of biomass into high value-added chemicals has become one of the most significant topics in 'green chemistry' in recent years. Extraction is the main way to obtain fine chemicals from biomass. However, these extraction processes suffer from several significant drawbacks, such as a demanding equipment, difficult purification, and high costs. To overcome these drawbacks, the development of chemical synthesis has become an important alternative method.

β -pinene oxide is a key intermediate in fine chemistry because it can undergo selective ring-opening reaction and rearrangement, obtaining a variety of scented, fragrant and antimicrobial chemicals. β -pinene oxide isomerization catalyzed by solid acid catalysts is one of the most efficient methods for obtaining the high value-added products (Figure 1) such as myrtanal, myrtenol and perillyl alcohol.^[1]

Most of the studies on the catalytic isomerization of β -pinene oxide^[2-6] have been directed toward the synthesis of myrtanal and myrtenol, which are used in the flavor and fragrance field. In general, perillyl alcohol occurs as a by-product of the isomerization of β -pinene oxide to myrtenol. Despite its antibacterial importance, only a few reports^[7,8] have investigated the selective synthesis of perillyl alcohol from β -pinene oxide. The highest reported yield of perillyl alcohol in

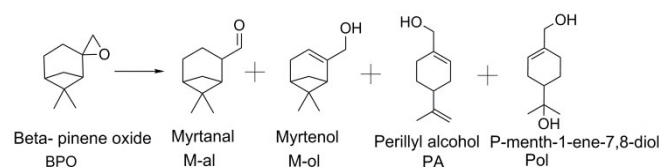


Figure 1. Reaction scheme of β -pinene oxide isomerization.

the isomerization of β -pinene oxide over solid acid catalysts is 66%, but achieving this yield takes a long time.^[9]

A pseudo-homogeneous method^[10,11] has the characteristics of "homogenized reaction, heterogenized recovery", which is of great significance to the industrial application of the catalyst. Recently, task-specific ionic compounds have attracted sustained attention^[12-18] due to their tailorable properties. Typically, this kind of compound is considered as a pseudo-homogeneous catalyst. For example, Di-cation imidazolium^[19,20] ionic liquids can achieve homogeneous catalytic reactions and heterogeneous separation by initially regulating its own structure. Based on the concept of such protic multi-cation arrays, we investigated protic tetraimidazolium salts with distinct and controllable backbone and different, in part protic anions as potential catalysts for β -pinene oxide isomerization. Thus far, there has been no published research literature on the highly selective synthesis of perillyl alcohol over imidazole ionic liquid catalysts by β -pinene oxide isomerization.

In this work, a series of tetracationic imidazolium salts with different anions was synthesized and successfully applied in the selective synthesis of perillyl alcohol by β -pinene oxide isomerization. The effect of different anions on the formation of the perillyl alcohol was proven, and the effect of different solvents on the product distribution was explored. Furthermore, the weak interaction between catalyst and solvent (DMSO) was studied by using computational chemistry and chemical characterization. Finally, a possible mechanism for the synthesis of perillyl alcohol by solvo-assisted catalysts was proposed.

[a] H. Li, J. Liu, J. Zhao, H. He, Dr. D. Jiang, Prof. S. R. Kirk, Prof. Q. Xu, Dr. X. Liu, Prof. D. Yin

National & Local Joint Engineering Laboratory for New Petro-chemical Materials and Fine Utilization of Resources
College of Chemistry and Chemical Engineering
Hunan Normal University
Changsha, 410081 (China)
E-mail: dulinyin@126.com

Supporting information for this article is available on the WWW under <https://doi.org/10.1002/open.202000318>

© 2021 The Authors. Published by Wiley-VCH GmbH. This is an open access article under the terms of the Creative Commons Attribution Non-Commercial License, which permits use, distribution and reproduction in any medium, provided the original work is properly cited and is not used for commercial purposes.

2. Results and Discussion

2.1. Catalyst Characterization

The imidazolium nitrate with different cations was analyzed by FT-IR. As shown in Figure 2, there are three characteristic vibration bands around 3103 cm^{-1} , 1632 cm^{-1} and 1385 cm^{-1} in all curves, which are respectively attributed to the characteristic vibration band of C–H on the imidazole ring, the characteristic vibration band of the imidazole ring skeleton and the stretching vibration band of N=O on the nitrate, indicating that three substances are ascribed to imidazole nitrate. In addition, as the number of imidazole ring increases, the intensity of the corresponding stretching vibration band also increases, which further confirms the synthesis of the imidazolium nitrate with different cations.

Tetraimidazolium ionic liquids with different anions were investigated by FT-IR. As shown in Figure 3, the characteristic bands (at around 3070 cm^{-1} , 1170 cm^{-1} and 1158 cm^{-1}) are associated with the stretching vibration mode of the tetraimidazolium moiety. The characteristic band at 620 cm^{-1} is associated

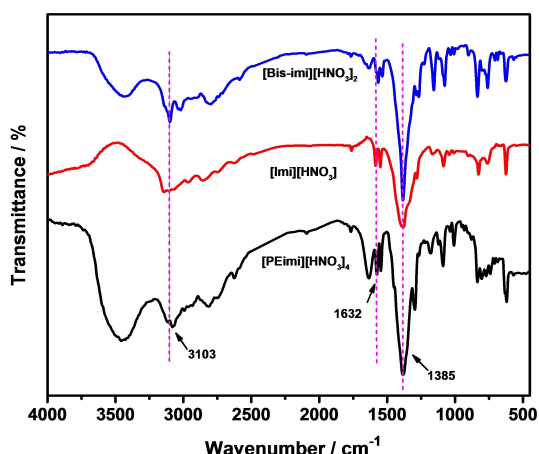


Figure 2. FT-IR spectra of [Imi][HNO₃], [Bis-im][HNO₃]₂ and [PEimi][HNO₃]₄.

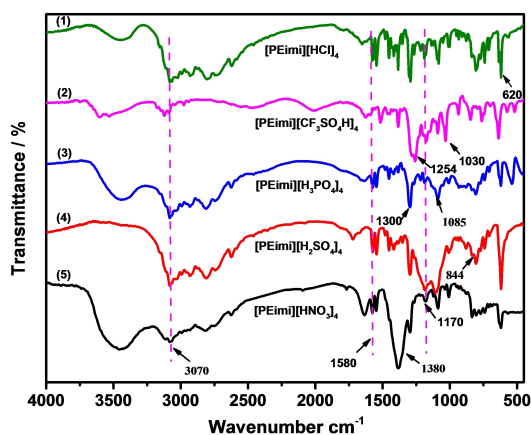


Figure 3. FT-IR spectra of (1) [PEimi][HCl]₄, (2) [PEimi][CF₃SO₄H]₄, (3) [PEimi][H₃PO₄]₄, (4) [PEimi][H₂SO₄]₄, (5) [PEimi][HNO₃]₄.

with the stretching vibration mode of C–Cl in curve(1), The characteristic bands at around 1245 cm^{-1} and 1030 cm^{-1} are associated, respectively, with the stretching vibration mode of C–F and S=O in CF₃SO₄[−] group in curve(2). The characteristic bands at around 1300 cm^{-1} and 1085 cm^{-1} are associated with the stretching vibration mode of P=O and P–O in H₂PO₄[−] group in curve(3). When the hydrogen sulfate is modified as the anion, the intensity of the stretching vibration band (at around 1170 cm^{-1}) is stronger than before, indicating that the characteristic band of stretching vibration of S=O in hydrogen sulfate coincides with the bending vibration band of C–H on imidazole ring. Additionally, The characteristic band at around 854 cm^{-1} is associated with the stretching vibration mode of S–O in HSO₄[−] group in curve(4). The characteristic band at around 1380 cm^{-1} is attributed to the stretching vibration mode of N–O in NO₃[−] group in curve(5).

¹H NMR spectroscopy was employed to gain further insight into the structural aspects of protic tetraimidazolium salts with different anions. As shown in Figure 4, it can be seen that the solubility of products of different anions in deuterium oxide is relatively different from the relative ratio of the characteristic peak to the solvent peak. The chemical shift of hydrogen atoms (at above 6 ppm) is associated with the type of hydrogen atom on the imidazole ring. After pentaerythryl tetraimidazole was neutralized with the corresponding acids to obtain tetraimidazolium salts with different anions, the chemical shifts of the corresponding hydrogen atoms on the imidazole ring are blue-shifted, indicating that the introduction of different anions produce corresponding weak interaction forces in catalysts, changing the chemical shift of hydrogen atoms in the raw materials.

The acid-base titration results were shown in Table 1. Considering the degree of ionization of anions in the catalysts, its theoretical protons value can be calculated. Comparing the above results, it is found that these protic imidazolium salts in water can be ionized to the protons to be equal to theoretical ones, suggesting that these imidazolium salts have great quality.

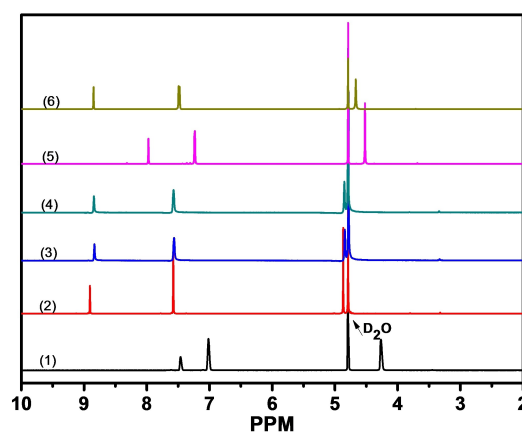


Figure 4. ¹H NMR spectra of (1) PEimi, (2) [PEimi][HNO₃]₄, (3) [PEimi][H₂SO₄]₄, (4) [PEimi][H₃PO₄]₄, (5) [PEimi][CF₃SO₄H]₄, (6) [PEimi][HCl]₄.

Table 1. The amount of H⁺ of different catalyst.

Entry	Catalyst	Amount [g]	Amount H ⁺ [mmol]	Determined H ⁺ [mmol]	Acid amount [mmol/g]
1	[Imi]HNO ₃	0.101	0.696	0.697	6.901
2	[Bis-imi][HNO ₃] ₂	0.100	0.365	0.366	3.660
3	[PEimi][HNO ₃] ₄	0.100	0.680	0.680	6.800
4	[PEimi][HCl] ₄	0.100	0.833	0.834	8.340
5	[PEimi][CF ₃ SO ₄ H] ₄	0.100	0.427	0.428	4.280
6	[PEimi][H ₂ SO ₄] ₄ ^[a]	0.102	1.120	1.100	10.784
7	[PEimi][H ₃ PO ₄] ₄ ^[b]	0.102	1.120	1.130	11.078

[a] H₂SO₄: pK_a⁰ = 1.99, [b] H₃PO₄: pK_a⁰ = 2.148, H₂PO₄⁻: pK_a⁰ = 7.198, HPO₄²⁻: pK_a⁰ = 12.32.

The Brønsted acidity of the catalyst was measured by UV-visible spectroscopy of the 4-Nitroaniline indicator (pK(I)_{aq} = 0.99), evaluating from the determination of the Hammett acidity functions. The detailed results are shown in Table 2. Notably, with the increase of imidazole moiety, the H₀ of the catalyst shows no noticeable change (Table S2, entry 2 vs. 3 and 4). Furthermore, the acidity of protic tetraimidazolium salts with different anions was investigated (Table S2, entry 4 vs. 5, 6, 7, and 8): the results indicated that the acidity of different catalysts follows the rules: [PEimi][HNO₃]₄ > [PEimi][CF₃SO₄H]₄ > [PEimi][H₂SO₄]₄. Considering that all the catalysts have better solubility in water, the Brønsted acidity of the catalyst was evaluated by Hammett functions of different acids in water. The

Table 2. Hammett functions of different Acids in DMSO.

Entry	Catalyst	Amax	[I] [%]	[IH ⁺] [%]	H ₀	H ₀ ^[a]
1	None	1.059	100.00	0.00	0.00	–
2	[Imi]HNO ₃	0.546	51.55	48.45	1.02	1.00
3	[Bis-imi][HNO ₃] ₂	0.511	48.23	51.77	0.96	0.99
4	[PEimi][HNO ₃] ₄	0.571	53.92	46.08	1.06	1.18
5	[PEimi][H ₂ SO ₄] ₄	0.617	58.26	41.74	1.13	0.95
6	[PEimi][H ₃ PO ₄] ₄	–	–	–	–	1.06
7	[PEimi][HCl] ₄	–	–	–	–	1.09
8	[PEimi][CF ₃ SO ₄ H] ₄	0.511	48.23	51.77	0.96	1.66

Indicator: 4-Nitroaniline (pK(I)_{aq} = 0.99), H₀ = pK(I)_{aq} + log([I]/[IH⁺]), [PEimi][H₃PO₄]₄ and [PEimi][HCl]₄ are insoluble in DMSO.
[a] H₀ is expressed as the Hammett functions of different acids in water.

Table 3. Effect of different catalysts on the isomerization of β-pinene oxide.

Entry	Catalyst	H ₀ ^[a]	Conv. [%]	TOF × 10 ⁻³ ^[b] [s ⁻¹]	Selectivity [%]				
					M-al	M-ol	PA	P-ol	Others
1	[Imi]HNO ₃	1.02	78.6	3.41	9.5	27.0	37.0	14.5	12.0
2	[Bis-imi][HNO ₃] ₂	0.96	94.8	4.11	7.1	24.5	44.2	15.8	8.4
3	[PEimi][HNO ₃] ₄	1.06	100.0	4.34	7.1	18.6	47.3	15.8	11.2
4	[PEimi][H ₂ SO ₄] ₄	1.13	85.1	3.69	8.8	20.6	37.7	12.4	20.5
5	[PEimi][H ₃ PO ₄] ₄	–	71.5	3.10	10.8	35.1	32.3	9.6	12.2
6	[PEimi][HCl] ₄	–	53.9	2.34	7.8	41.3	29.2	8.3	13.5
7	[PEimi][CF ₃ SO ₄ H] ₄	1.09	99.6	4.32	8.1	22.4	43.6	16.7	9.3

Reaction conditions: Catalyst (4.8 mol% β-pinene oxide), β-pinene oxide (5 mmol), DMSO (2.5 ml), 80 min, 40 °C.
[a] H₀ is represented as Hammett functions of different acids in DMSO: [PEimi][H₃PO₄]₄ and [PEimi][HCl]₄ are insoluble in DMSO.
[b] TOF is calculated by the $TOF = \frac{\text{moles of BPO}}{\text{moles of catalyst} \times \text{time}} \text{ (s}^{-1}\text{)}$

results show the Brønsted acidity of all catalysts can be given, which is different from the acidity of catalysts in DMSO.

2.2. Catalytic Performance

The catalytic performance of different catalysts in the selective synthesis of perillyl alcohol by β-pinene oxide isomerization, is summarized in Table 3. Notably, with the increase of imidazole moiety, the yield of perillyl alcohol has significantly increased (Table 1, entry 1 vs. 2 and 3), indicating that multi-cation imidazolium plays an important role in facilitating the multi-active sites of Brønsted acid, which can accelerate to form more C6 product in the rearrangement of β-epoxide pinene. Furthermore, the effect of tetraimidazolium with different anions was investigated (Table 1, entry 3 vs. 4, 5, 6, and 7): the results showed that the catalytic activity of different catalysts follows the following rules: [PEimi][HNO₃]₄ > [PEimi][CF₃SO₄H]₄ > [PEimi][H₂SO₄]₄ > [PEimi][H₃PO₄]₄ > [PEimi][HCl]₄, which was consistent with the acidic strength of the catalysts. In summary, we selected [PEimi][HNO₃]₄ as the optimum catalyst for catalytic performance in the selective synthesis of Perillyl alcohol by β-pinene oxide isomerization. In addition, the [PEimi][HNO₃]₄ has a very good thermal stability by TG-DTG analysis: for details see Fig. S1 (see ESI+).

Given that the reaction solvent plays a critical role in the catalytic performance of the [PEimi][HNO₃]₄ in the synthesis of perillyl alcohol by β-pinene oxide isomerization, Table 4 shows in detail the comparative results of the isomerization of β-pinene oxide over [PEimi][HNO₃]₄ in various solvents. It was found that the non-polar toluene has high conversion with low selectivity of perillyl alcohol. An the increase of the solvent polarity, such as chloroform, ethyl acetate and acetone, used for the isomerization of β-pinene oxide, results in low conversion and more by-products. The difference should be associated with the expectation that the high polar catalyst is easily dissolved in a solvent of similar polarity, avoiding the problem of mass transfer obstruction. In addition, although the catalyst can be well dissolved in methanol, the results indicate that the reaction was completely transformed and yield more of the isomers of perillyl alcohol. Furthermore, 28.6% selectivity of perillyl alcohol was obtained in nitromethane: this can be attributed to the weakly basic nature of the solvent, which

Table 4. Effect of solvent polarity on the isomerization of β -pinene oxide.

Solvent	Dielectric constant	Conv. [%]	TOF $\times 10^{-3}$ [s ⁻¹] ^[a]	Selectivity [%]				
				M-al	M-ol	PA	P-ol	Others
Toluene	2.38	62.0	2.69	14.0	14.6	9.6	0.4	61.4
Trichloromethane	4.70	30.9	1.34	10.3	17.5	7.8	2.3	62.1
Ethyl acetate	6.03	37.9	1.64	13.8	12.1	8.6	1.8	63.7
Acetone	20.5	34.3	1.49	11.1	16.0	8.2	1.9	62.8
Methanol	32.6	99.9	4.33	2.8	8.4	12.2	14.0	62.6
Nitromethane	38.6	51.8	2.25	6.8	15.1	28.6	2.7	46.8
DDimethyl sulfoxide(DMSO)	48.9	100.0	4.34	7.1	18.6	47.3	15.8	11.2

Reaction conditions: Catalyst (4.8 mol% β -pinene oxide), β -pinene oxide (5 mmol), solvent (2.5 ml), 80 min, 40 °C.

[a] TOF is calculated by the $TOF = \frac{\text{moles of BPO}}{\text{moles of catalyst} \times \text{time}} \text{ (s}^{-1}\text{)}$.

promotes ring-opening for the formation of C6 products. The dimethyl sulfoxide (DMSO) was the optimal solvent for the isomerization of β -pinene oxide, obtaining an excellent yield of perillyl alcohol due to the high polarity and weakly basic solvent.^[4]

In the next experiment, the effect of reaction temperature and reaction time in the synthesis of perillyl alcohol by β -pinene

oxide isomerization was studied. As shown in Figure 5, the results showed that the conversion rate of β -pinene oxide gradually increases with increasing temperature. When the temperature reaches 40 °C, the reaction is completed. As the reaction temperature continues to increase, more perillyl alcohol is generated at the expense of myrtenal and myrtenol formation. The remarkable change in the trend of the product distribution might be due to the product of a reaction under thermodynamic control.^[8] As shown in Figure 6, with the increase of reaction time from 20 to 80 min, the conversion of β -pinene oxide shows an obvious increase from 67% to 95% with over 44% selectivity for perillyl alcohol. Upon further extending the reaction time, the selectivity for perillyl alcohol increases slightly. Furthermore, the product distribution follows a rule that a significant increase in the selectivity to perillyl alcohol occurs at the expense of myrtenol and myrtenal formation during the whole reaction time. This might be due to the reaction system being more favorable toward generation of more perillyl alcohol over the catalysis for a long time.

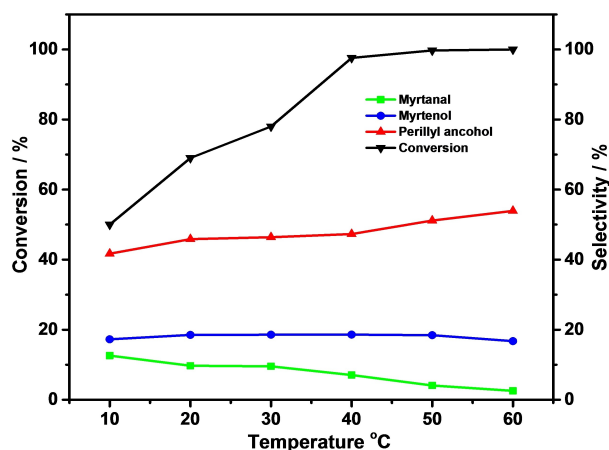


Figure 5. Effect of temperature on the isomerization of β -pinene oxide.

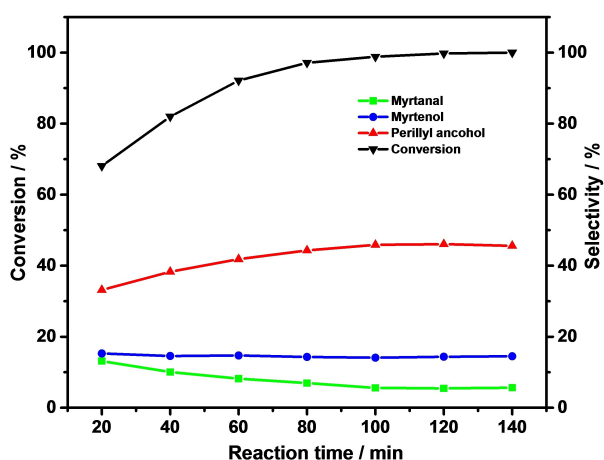


Figure 6. Effect of reaction time on the isomerization of β -pinene oxide.

2.3. Catalyst Reusability

Although the [PEimi][HNO₃]₄ is used in a reaction as a homogeneous catalyst, it can be easily recovered from the reaction mixture by adjusting the polarity of the solvent system: it was added in a large amount of ethyl acetate, centrifuged, washed with ethyl acetate and reused. Figure 7 shows the results of the recyclability of [PEimi][HNO₃]₄ in the synthesis of perillyl alcohol by β -pinene oxide isomerization. It was gratifying to observe that; the catalyst could be reused six times without a significant decrease in the conversion and selectivity of perillyl alcohol. In addition, the reused catalyst was characterized by ¹H NMR and FT-IR, as shown in Figure 8–9. The results suggested that the reused catalyst still maintained its original structure, indicating that [PEimi][HNO₃]₄ exhibits great stability and recyclability.

2.4. Microscopic Interaction Between Solvent and Catalyst

In order to visually investigate the microscopic interaction between solvent and catalyst, a few catalysts were dissolved in

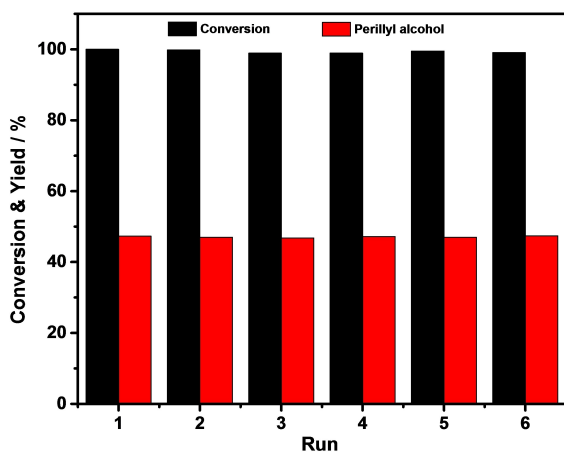


Figure 7. Recyclability of [PEimj][HNO₃]₄ on the isomerization of β -pinene oxide.

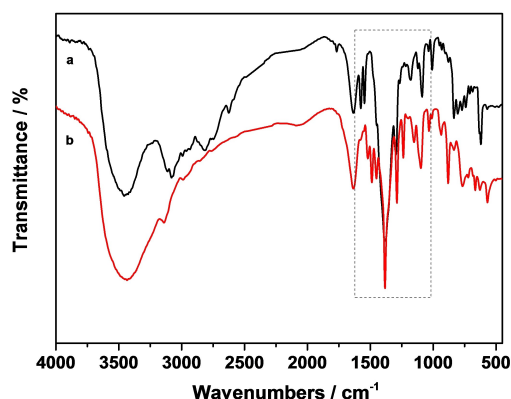


Figure 8. FT-IR spectra of fresh (a) and reused (b) of [PEimj][HNO₃]₄.

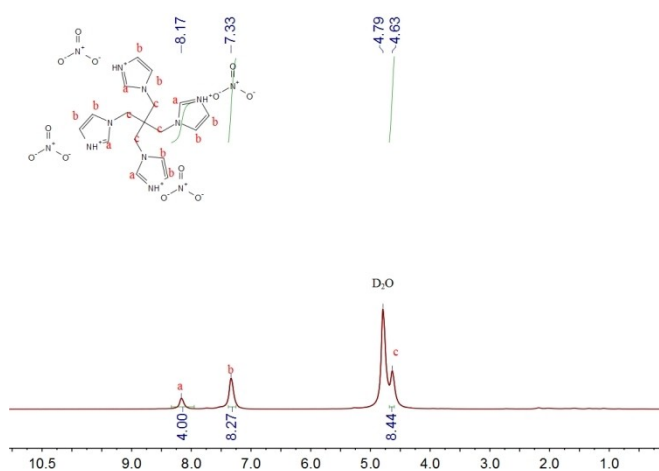


Figure 9. ¹H NMR of reused [PEimj][HNO₃]₄.

dimethyl sulfoxide-D₆ to simulate the actual catalytic system: the sample and blank were measured using FT-IR spectra. The detailed results are shown in Figure 10. The characteristic vibration bands of C–D in DMSO-D₆ at around 2125.37 and

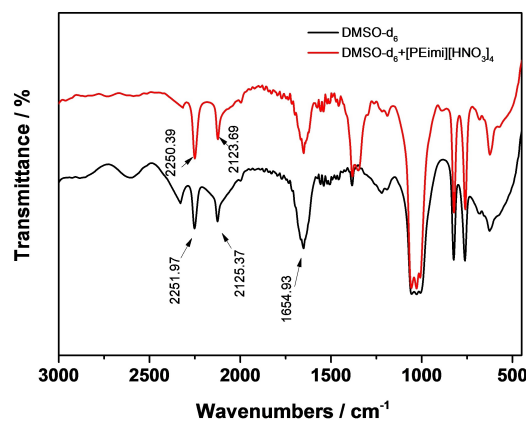


Figure 10. FT-IR spectra of DMSO-d₆ and DMSO-D₆ + [PEimj][HNO₃]₄.

2251.97 cm⁻¹. After adding the catalyst, the band corresponding to the C–D in DMSO-D₆ was slightly displaced, and the characteristic bands of C²-H in imidazole ring groups (at around 1630 cm⁻¹) have a significant red shift, indicating the generation of hydrogen bonds between C²-H (in catalyst) and S=O in DMSO-D₆. Furthermore, we used computational chemistry to further illustrate the weak interaction between the catalyst and solvent. Considering the catalyst itself as a symmetric structure, using explicit basic units and restricted computing devices, the structure of catalyst was calculated by using basic units instead of catalyst, as shown in Figure 11.

In order to visualize the noncovalent interaction between solvent and catalyst, we thereby using the reduced density gradient (RDG)^[21] to examine such effect. The geometrical calculation was optimized under density functional theory M06-2X^[22] with Ahlrichs' triple-zeta basis sets def-TZVP,^[23] following tight SCF convergence and ultrafine integration grids, by using the Gaussian 09^[24] package, version B01. The Multiwfn 3.7 program^[25] was employed to do RDG calculations using the formatted checkpoint file generated from Gaussian calculation as the inputs. The gradient isosurface can be colored according to the sign(λ_2) values in plot of RDG, which is a straight illustration of noncovalent interaction between solvent molecule and catalyst. Figure 12 shows in detail the results of gradient isosurface (a) and scatter plot of the RDG (b) for one

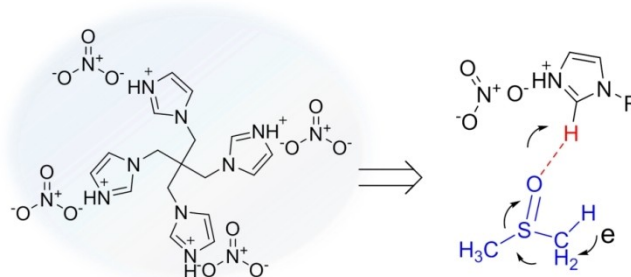


Figure 11. The weak interaction between the basic unit of the catalyst and DMSO.

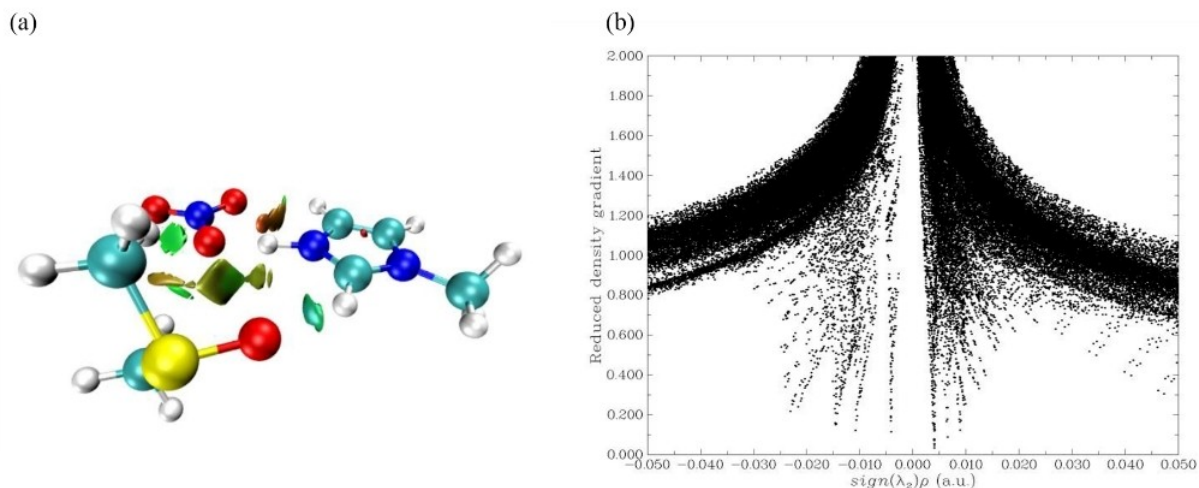
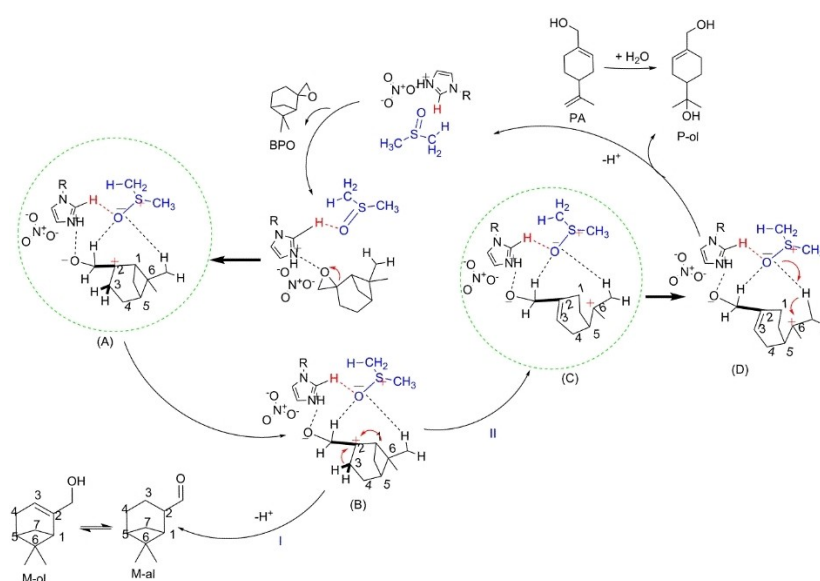


Figure 12. Reduced density gradient versus the electron density multiplied by the sign of the second Hessian eigenvalue, data evaluated at M06-2X/def-TZVP level of theory.

basic unit of the catalyst and DMSO. According to the values of $\text{sign}(\lambda_2)\rho$,^[26] ranging from -0.05 to 0.05 au., the gradient isosurfaces are colored on a blue-green-red scale, which respectively indicates strong attractive interactions (hydrogen bonds), Van der Waals force and strong non-bonded overlap (strong site-resistance effects). Thus, the results clearly show the evidence for the hydrogen bond between the S=O (in the DMSO group) and C²-H (on the imidazole ring).^[27–29] Same results could also be evaluated from the 2D plot (b), where the most spikes are lying at negative values suggesting that some interactions are playing a stabilizing role in the system.

2.5. Proposed Mechanism

A plausible mechanism of acid-catalyzed transformations of β -pinene oxide is presented in Scheme 1. A tertiary carbocation (A) is formed by protonation of the exo-epoxide with H⁺ released by the imidazole ring in [PEimi][HNO₃]₄. Transformation of the tertiary carbocation (A) results in two reaction paths (I) and (II) due to the polarity and basicity of solvent. In path (I), the electron pair quickly transfer from C³ by proton release giving myrtenol (M-ol) and myrtenal (M-al). On the other hand, the hydrogen bond between the S=O (in DMSO group) and C²-H (on the imidazole ring) can further stabilize the catalyst. In path (II), the tertiary carbocation (A) can involve the same electron pair. However, the DMSO as a solvent with high



Scheme 1. Plausible mechanism of acid-catalyzed transformations of β -pinene oxide.

polarity and basicity, can facilitate the deprotonation of the C–C bond. Thus, the allylic carbocation (C) is formed via the breaking of the C¹–C⁶ bond in (B) and the deprotonation of C³. Subsequently, the proton is released to obtain perillyl alcohol; in addition, the presence of a small amount of residual water is sufficient to favor the formation of P-ol.

3. Conclusion

In this work, a series of tetraimidazolium salts with different anions was successfully synthesized by simple nucleophilic substitution and neutralization and used in the synthesis of perillyl alcohol by β -pinene oxide isomerization. Among the different catalysts examined, [PEimi][HNO₃]₄, as a pseudo homogeneous catalyst, exhibits remarkable yield of perillyl alcohol (47%) under the mild reaction conditions of 5 mmol of β -pinene oxide, 2.5 ml of DMSO as solvent, 4.8 mol% catalyst, 40 °C and 80 min. Importantly, the catalyst was reused in six runs without a significant loss, being recovered by a simple centrifuge. Moreover, the weak interaction between catalyst and solvent (DMSO) was studied theoretically and experimentally, providing evidence for an imidazole-buffered acid-base mechanism.

Experimental Section

Materials and Reagents

Imidazole, 1-methylimidazole, sodium hydroxide, toluene, dimethyl sulfoxide, dibromomethane, nitric acid, sulfuric acid, trifluoromethanesulfonic acid, phosphoric acid, 4-Nitroaniline, acetone and methanol were AC grade purchased from Sinopharm Chemical Reagent Co., Ltd. Pentaerythrityl tetrabromide were AC grade purchased from Alfa Aesar.

Methods

The structure of the materials was characterized by using Fourier transform infrared (FT-IR) spectra. These were measured using KBr pellets with a resolution of 4 cm⁻¹ and 32 scans in the range of 400–4000 cm⁻¹ using a Nicolet Nexus 670 spectrometer. NMR spectra data were obtained on a Bruker Avance-500 MHz spectrometer with tetrakis (trimethylsilyl) silane (TMS) as the internal standard. Thermogravimetric and differential thermogravimetric (TG-DTG) curves were recorded on a Netzsch-STA409PC thermalgravimetric analyzer, and the samples were heated from 30 °C to 800 °C with 10 K min⁻¹ under nitrogen flow.

The acidity of the materials was evaluated by a traditional acid-base titration. Samples 0.1 g were dissolved in 25 ml distilled water and titrated by the calibrated 0.01 mol/L NaOH solution with phenolphthalein as an indicator. The average titration result is considered as the acid amount of the catalyst. UV-visible spectroscopy measurements were recorded on a UV-vis Agilent 8453 spectrophotometer with 4-Nitroaniline (pK(l)aq = 0.99) as the indicator and using the method of Hammett acidity functions.^[30]

Preparation of the Imidazole Skeleton

Synthesis of gemini imidazole. imidazole (6.816 g, 0.1 mol), KOH (6.732 g, 0.12 mol) were stirred in methanol (100 ml) at 50 °C for 1 h. After removing methanol, dibromomethane (8.592 g, 0.05 mol) and tetrabutyl ammonium bromide (0.1 g) were slowly added and stirred in acetonitrile (100 ml) at 80 °C for 6 h. The reaction mixture was filtered to remove potassium bromide, the filtrate was cyclically steamed to remove the solvent, The crude product was recrystallized with acetone at a yield of 31.3%.

¹H NMR (500 MHz, DMSO) δ 7.93 (s, 2H), 7.39 (s, 2H), 6.91 (s, 2H), 6.21 (s, 2H); ¹³C NMR (126 MHz, CDCl₃) δ 136.62 (s), 131.19 (s), 118.12 (s), 77.30 (s), 77.05 (s), 76.79 (s), 56.35 (s); Elem. Anal.(calc.): C, 56.73 (56.74); H, 5.42 (5.44); N, 37.85 (37.81).

Synthesis of pentaerythrityl tetraimidazole.^[31,32] Imidazole (6.816 g, 0.1 mol) was dissolved in toluene(12 ml) and dimethyl sulfoxide (12 ml), 50% sodium hydroxide(16 g) was slowly added dropwise and stirred at room temperature for 30 min, then heated to 110 °C until the generated water was removed. Pentaerythrityl tetrabromide (7.672 g, 0.02 mol) was added slowly, then the reaction mixture was heated to 110 °C for 4 h, then filtered to remove sodium bromide. The filtrate was poured into a large amount of ice water, The crude product was obtained after sitting at room temperature overnight. After filtration, the product was washed with pure water and dried at 65 °C vacuum for 12 h. The white solid was obtained with a yield of 26%.

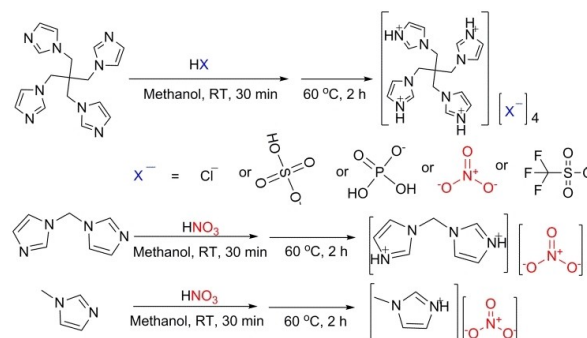
¹H NMR (500 MHz, DMSO) δ 7.49 (s, 4H), 6.97 (s, 4H), 6.93 (s, 4H), 4.16 (s, 8H); ¹³C NMR (126 MHz, DMSO) 139.44 (s), 129.36 (s), 121.60 (s), 49.84 (s), 42.51(s). Elem. Anal.: C,60.70; H,5.99; N,33.31.

Preparation of Catalyst

The synthesis of the imidazolium, Di-cation imidazolium and tetracation imidazolium salts is presented in Scheme 2. The specific synthesis steps were similar, the structure and denominate of catalyst was presented in Table S1.

Preparation of tetracation imidazolium nitrate as an example: pentaerythrityl tetraimidazole (1 mmol) was dissolved in methanol (10 ml), then nitric acid (4 mmol) was added slowly under the ice bath. The mixture was stirred at room temperature for 1 h, then heated to 60 °C for 2 h. The product was obtained by removing the methanol, then drying overnight at 70 °C under vacuum.

[Imi][HNO₃]: ¹H NMR (500 MHz, D₂O) δ 8.64 (s, 1H), 7.42 (s, 2H), 3.91 (s, 3H), ¹³C NMR (126 MHz, D₂O) δ 134.97 (s), 122.93 (s), 119.44 (s), 35.38 (s), 20.93 (s). Elem. Anal.: C, 33.12 (33.11); H, 4.87 (4.86); N, 28.98(28.96); O,33.03 (33.07).



Scheme 2. Synthesis of protic imidazolium salts.

[Bis-im][HNO₃]₂: ¹H NMR (500 MHz, D₂O) δ 9.18 (s, 2H), 7.75 (s, 2H), 7.56 (s, 2H), 6.74 (s, 2H); ¹³C NMR (126 MHz, D₂O) δ 136.23 (s), 121.39 (s), 121.12 (s), 58.66 (s). Elem. Anal.: C, 30.65 (30.66); H, 3.67 (3.68); N, 30.66 (30.65); O, 35.02 (35.01).

[PEimi][HNO₃]₄: ¹H NMR (500 MHz, D₂O) δ 8.91 (s, 4H), 7.58 (s, 8H), 4.87 (s, 8H); ¹³C NMR (126 MHz, D₂O) δ 136.86 (s), 123.04 (s), 121.36 (s), 50.69 (s), 42.16 (s); Elem. Anal.(calc.): C, 34.73 (34.70); H, 4.15 (4.11); N, 28.47 (28.56); O, 32.65 (32.63).

[PEimi][H₂SO₄]₄: ¹H NMR (500 MHz, D₂O) δ 8.94 (s, 4H), 7.57 (s, 8H), 4.87 (s, 8H); ¹³C NMR (126 MHz, D₂O) δ 136.83 (s), 123.06 (s), 121.27 (s), 50.76 (s), 42.01 (s); Elem. Anal.: C, 28.04 (28.02); H, 3.88 (3.87); N, 15.40 (15.38); O, 35.11 (35.13); S, 17.57 (17.63).

[PEimi][H₃PO₄]₄: ¹H NMR (500 MHz, D₂O) δ 8.84 (s, 4H), 7.57 (s, 8H), 4.85 (s, 8H); ¹³C NMR (126 MHz, D₂O) δ 136.78 (s), 122.97 (s), 121.54 (s), 50.70 (s), 42.02 (s); Elem. Anal.: C, 28.02 (28.03); H, 4.40 (4.43); N, 15.40 (15.38); O, 35.16 (35.14); P, 17.02 (17.07).

[PEimi][HCl]₄: ¹H NMR (500 MHz, D₂O) δ 8.85 (s, 4H), 7.48 (d, J = 9.1 Hz, 8H), 4.67 (s, 8H); ¹³C NMR (126 MHz, D₂O) δ 136.81 (s), 123.12 (s), 121.35 (s), 50.77 (s), 42.15 (s); Elem. Anal.: C, 42.31 (42.34); H, 5.03 (5.02); N, 23.22 (23.24); Cl, 29.44 (29.40).

[PEimi][CF₃SO₃H]₄: ¹H NMR (500 MHz, D₂O) δ 8.94 (s, 4H), 7.57 (s, 8H), 4.87 (s, 8H); ¹³C NMR (126 MHz, D₂O) δ 136.83 (s), 123.06 (s), 121.27 (s), 50.76 (s), 42.01 (s); Elem. Anal.: C, 26.95 (26.93); H, 2.57 (2.58); N, 11.95 (11.96); O, 20.47 (20.50); S, 13.70 (13.69); F, 24.36 (24.34).

Catalyst Testing

The isomerization reaction was carried out in a 10 ml magnetically stirred round-bottom flask. In a typical experiment, the catalyst (5 mol% β-pinene oxide), β-pinene oxide (5 mmol) and solvent (2.5 ml) were added into the flask. The reaction was stirred at 40 °C for 80 min. After that, the products were measured by a gas chromatograph (Shimadzu GC 2014, Japan) with HP-5 column (30.0 m × 0.50 mm × 0.32 μm) and verified by GC-MS (Shimadzu GCMS-QP2010, Japan). Test Conditions: the carrier gas was N₂, the split was 40:1, the column temperature was 130 °C for 20 min. Because the response factor of the isomerization products was similar to the β-Pinene epoxide, and the polymerization products were not detected, normalization of areas was used to quantify the conversion of the substrates and the selectivity of the products. The catalyst was recovered by adjusting the polarity of the solvent system: it was poured in a large amount of ethyl acetate until the solution remained cloudy, then centrifuged, washed with ethyl acetate and reused. The catalyst activity was evaluated from the conversion of β-pinene oxide (BPO) and the selectivity of perillyl alcohol (PA), which is defined as follows:

$$\text{BPO Conversion (\%)} = \frac{\text{moles of reacted BPO}}{\text{moles of added BPO}} \times 100$$

$$\text{PA Selectivity (\%)} = \frac{\text{moles of PA}}{\text{moles of reacted BPO}} \times 100$$

$$\text{TOF (S}^{-1}\text{)} = \frac{\text{moles of BPO}}{\text{moles of catalyst} \times \text{reaction time}}$$

Acknowledgements

We acknowledge the financial support for this study by the National Natural Science Foundation of China (Grant Nos. 21975070, 21776068).

Conflict of Interest

The authors declare no conflict of interest.

Keywords: tetraimidazolium salts · green chemistry · isomerization reactions · Perillyl alcohol · homogeneous catalysis

- [1] S. Shojaei, A. Kiumarsi, A. R. Moghadam, J. Alizadeh, H. Marzban, S. Ghavami, *Natural Products and Cancer Signaling: Isoprenoids, Polyphenols and Flavonoids*, F. Tamanoi, S. Bathaie, **2014**, pp. 12.
- [2] O. D. L. Torre, M. Renz, A. Corma, *Appl. Catal. A* **2010**, *380*, 165–171.
- [3] L. V. Il'ina, S. Y. Kurbakova, K. P. Volcho, N. F. Salakhutdinov, V. I. Anikeev, *J. Saudi Chem. Soc.* **2011**, *15*, 313–317.
- [4] P. Mäki-Arvela, N. Kumar, S. F. Díaz, A. Aho, M. Tenho, J. Salonen, A. R. Leino, K. Kordás, P. Laukkanen, J. Dahl, I. Sinev, T. Salmi, D. Y. Murzin, *J. Mol. Catal. A* **2013**, *366*, 228–237.
- [5] E. Salminen, L. Rujana, P. Mäki-Arvela, P. Virtanen, T. Salmi, J. P. Mikkola, *Catal. Today* **2015**, *257*, 318–321.
- [6] J. E. Sánchez-Velandia, A. L. Villa, *Appl. Catal. A* **2019**, *580*, 17–27.
- [7] E. Vyskočilová, M. Malý, A. Aho, J. Krupka, L. Červený, *React. Kinet. Mech. Catal.* **2016**, *118*, 235–246.
- [8] J. E. Sánchez-Velandia, J. F. Gelves, L. Dorkis, M. A. Márquez, A. L. Villa, *Microporous Mesoporous Mater.* **2019**, *287*, 114–123.
- [9] Q. H. Li, L. L. Kuang, H. J. Yuan, *J. Nat. Sci. Hunan Normal Univ.* **2008**, *31*, 74–77.
- [10] V. Umrigar, M. Chakraborty, P. Parikh, *Int. J. Chem. Kinet.* **2019**, *51*, 299–308.
- [11] M. Banchemo, G. Gozzelino, *Energies*. **2018**, *11*, 1843–1855.
- [12] A. S. Amarasekara, *Chem. Rev.* **2016**, *116*, 6133–6183.
- [13] C. Y. Li, J. F. Zhao, R. Tan, Z. G. Peng, R. C. Luo, M. Peng, D. H. Yin, *Catal. Commun.* **2011**, *15*, 27–31.
- [14] R. Tan, C. Y. Li, Z. G. Peng, D. L. Yin, D. H. Yin, *Catal. Commun.* **2011**, *12*, 1488–1491.
- [15] R. Tan, C. Y. Li, J. Q. Luo, Y. Kong, W. G. Zheng, D. H. Yin, *J. Catal.* **2013**, *298*, 138–147.
- [16] Q. Wang, Z. M. Wu, Y. F. Li, Y. Tan, N. Liu, Y. J. Liu, *RSC Adv.* **2014**, *4*, 33466–33473.
- [17] J. F. Xiao, H. Huang, W. J. Xiang, W. Liao, J. Y. Liu, X. C. She, Q. Xu, Z. H. Fu, S. R. Kirk, D. L. Yin, *RSC Adv.* **2016**, *6*, 92716–92722.
- [18] D. F. Wang, Z. C. He, Z. M. Wu, Y. Tan, Y. F. Li, Y. J. Liu, *Chin. J. Chem. Eng.* **2016**, *24*, 1166–1170.
- [19] Z. C. He, Z. M. Wu, Y. F. Li, Q. Wang, L. S. Pan, Y. J. Liu, *J. Mole. Catal. (China)* **2014**, *28*, 536–543.
- [20] Y. D. Zhang, G. J. Chen, L. Wu, K. Liu, H. Zhong, Z. Y. Long, M. M. Tong, Z. Z. Yang, S. Dai, *Chem. Commun.* **2020**, *56*, 3309–3312.
- [21] E. R. Johnson, S. H. Keinan, P. Mori-Sanchez, J. Contreras-Garci'a, A. J. Cohen, W. T. Yang, *J. Am. Chem. Soc.* **2010**, *132*, 6498–6506; a, A. J. Cohen, W. T. Yang, *J. Am. Chem. Soc.* **2010**, *132*, 6498–6506.
- [22] Y. Zhao, D. G. Truhlar, *Theor. Chem. Acc.* **2007**, *120*, 215–241.
- [23] A. Schäfer, C. Huber, R. Ahlrichs, *J. Chem. Phys.* **1994**, *100*, 5829–5835.
- [24] M. J. Frisch, G. W. Trucks, H. B. Schlegel, G. E. Scuseria, M. A. Robb, J. R. Cheeseman, G. Scalmani, V. Barone, G. A. Petersson, H. Nakatsuji, X. Li, M. Caricato, A. Marenich, J. Bloino, B. G. Janesko, R. Gomperts, B. Mennucci, H. P. Hratchian, J. V. Ortiz, A. F. Izmaylov, J. L. Sonnenberg, D. Williams-Young, F. Ding, F. Lipparini, F. Egidi, J. Goings, B. Peng, A. Petrone, T. Henderson, D. Ranasinghe, V. G. Zakrzewski, J. Gao, N. Rega, G. Zheng, W. Liang, M. Hada, M. Ehara, K. Toyota, R. Fukuda, J. Hasegawa, M. Ishida, T. Nakajima, Y. Honda, O. Kitao, H. Nakai, T. Vreven, K. Throssell, J. A. Montgomery, Jr., J. E. Peralta, F. Ogliaro, M. Bearpark, J. J. Heyd, E. Brothers, K. N. Kudin, V. N. Staroverov, T. Keith, R. Kobayashi, J. Normand, K. Raghavachari, A. Rendell, J. C. Burant, S. S.

- Iyengar, J. Tomasi, M. Cossi, J. M. Millam, M. Klene, C. Adamo, R. Cammi, J. W. Ochterski, R. L. Martin, K. Morokuma, O. Farkas, J. B. Foresman, D. J. Fox, *Gaussian, Inc., Wallingford CT*, 2016.
- [25] T. Lu, F. Chen, *J. Comput. Chem.* **2012**, *33*, 580–592.
- [26] S. G. Mohamed-Hussain, R. Kumar, M. Mohamed Naseer Ali, B. Shanmugapriyan, V. Kannappan, *J. Mol. Liq.* **2020**, *297*, 111906.
- [27] Y. Chu, H. Deng, J. P. Cheng, *J. Org. Chem.* **2007**, *72*, 7790–7793.
- [28] P. A. Hunt, B. Kirchner, T. Welton, *Chem. Eur. J.* **2006**, *12*, 6762–6775.
- [29] C. Chen, X. Y. Wang, J. Yao, K. X. Chen, Y. Guo, P. F. Zhang, H. R. Li, *ChemPhysChem* **2015**, *16*, 3836–3841.
- [30] C. Thomazeau, H. Olivier-Bourbigou, Magna, L. Magna, S. Luts, B. Gilbert, *J. Am. Chem. Soc.* **2003**, *126*, 5264–5265.
- [31] H. Y. Liu, D. M. Gu, G. Y. Liu, X. L. Zhao, C. Chen, *Procedia Eng.* **2011**, *18*, 324–328.
- [32] Y. G. Yuan, Y. Zhang, *ChemMedChem* **2017**, *12*, 835–840.

Manuscript received: November 3, 2020
Revised manuscript received: February 17, 2021